Carbohydrate Polymers 113 (2014) 403–410

Contents lists available at ScienceDirect

Carbohydrate Polymers

journal homepage: www.elsevier.com/locate/carbpol

Enhanced thermal and mechanical properties of PVA composites formed with filamentous nanocellulose fibrils

Wei Li[a,b], Qiong Wu[a], Xin Zhao[a], Zhanhua Huang[a], Jun Cao[b], Jian Li[a,*], Shouxin Liu[a,*]

[a] Material Science and Engineering College, Northeast Forestry University, Harbin 150040, China
[b] College of Mechanical and Electrical Engineering, Northeast Forestry University, Harbin 150040, China

ARTICLE INFO

Article history:
Received 16 April 2014
Received in revised form 28 May 2014
Accepted 9 July 2014
Available online 22 July 2014

Keywords:
Nanocellulose fibrils
CTMP
Ultrasonication
Poly(vinyl alcohol)

ABSTRACT

Long filamentous nanocellulose fibrils (NCFs) were prepared from chemical-thermomechanical pulps (CTMP) using ultrasonication. Their contribution to enhancements in thermal stability and mechanical properties of poly(vinyl alcohol) films were investigated. The unique chemical pretreatment and mechanical effects of CTMP loosen and unfold fibers during the pulping process, which enables further chemical purification and subsequent ultrasound treatment for formation of NCFs. The NCFs exhibited higher crystallinity (72.9%) compared with that of CTMP (61.5%), and had diameters ranging from 50 to 120 nm. A NCF content of 6 wt% was found to yield the best thermal stability, light transmittance, and mechanical properties in the PVA/NCF composites. The composites also exhibited a visible light transmittance of 73.7%, and the tensile strength and Young's modulus were significantly improved, with values 2.8 and 2.4 times larger, respectively, than that of neat PVA.

1. Introduction

Natural fiber-reinforced polymer composites are a potential solution for the environmental burden presented by the use of petroleum-based, non-biodegradable polymeric materials (Pandey, Misra, Mohanty, Drzal, & Singh, 2005; Svagan, Samir, & Berglund, 2008; Shih & Huang, 2011). Nanocellulose fibrils (NCFs) are ideal candidates for reinforced composites owing to their abundance, renewability, biodegradability, exceptional mechanical properties (high specific strength and modulus), low thermal expansion, environmental benefits, and low cost (Habibi, Lucia, & Rojas, 2010; Wegner & Jones, 2006; Zhang, Zhang, Lu, & Deng, 2012; Bhatnagar & Sain, 2005; Abdul Khalil, Bhat, & Ireana Yusra, 2012).

The isolation of NCFs from cellulose fibers using simple, low cost, and environmentally friendly methods is a great challenge (Phong, Gabr, Okubo, Chuong, & Fujii, 2013; Wang & Cheng, 2009). Several mechanical processes have been used to extract nanofibers from cellulosic materials, such as pulping beating (Nakagaito & Yano, 2004; Chakraborty, Sain, & Kortschot, 2005), high pressure homogenizing (Bruce, Hobson, Farrent, & Hepworth, 2005; Stenstad, Andresen, Tanem, & Stenius, 2008; Leitner, Hinterstoisser, Wastyn, Keches, & Gindl, 2007), and cryogenic crushing (Alemdar & Sain, 2008; Wang & Sain, 2007).

Recently, ultrasonic techniques have been used to isolate cellulose nanofibers (Chen, Yu, & Liu, 2011a; Cheng, Wang, & Han, 2010; Cheng, Wang, & Rials, 2009). They apply sound energy to disrupt physical and chemical systems, and ultrasonication-induced cavitation for degrading polysaccharide linkages, such as chitosan (Liu, Du, & Kennedy, 2007; Kasaai, Arul, & Charlet, 2008), dextran (Cote & Willet, 1999; Portenlanger & Heusinger, 1997), xyloglucan (Vodeniãarová, Drímaloví, Hromádková, Malovíková, & Ebringerová, 2006), and carboxymethylcellulose (Gronroos, Pirkonen, & Ruppert, 2004; Aliyu & Hepher, 2000) has been well documented. Moreover, the violent collapse during cavitation creates micro-jets and shock waves on the surface of purified cellulose fibers, causing erosion and splitting along the axial direction. Sonification can break the relatively weak nonbonding interactions, such as van der Waals forces, at the interfaces between the microfibers (Suslick, Choe, Cichowlas, & Grinstaff, 1991; Filson & Dawson-Andoh, 2009; Zhao, Feng, & Gao, 2007). Thus, ultrasonication is well suited for isolating NCFs having relatively long networks (Cheng et al., 2009; Tischer, Sierakowski, Westfahl, & Tischer, 2010).

High-intensity ultrasonication, combined with chemical pretreatments, has been used to prepare NCFs from several raw materials, such as bamboo, wood, microcrystalline cellulose (MCC)

* Corresponding authors at: Material Science and Engineering College, Northeast Forestry University, Harbin 150040, China.
Tel.: +86 451 82192399/+86 451 82191204;
fax: +86 451 82192399/+86 451 82191204.
E-mail addresses: nefulijian@163.com (J. Li), liushouxin@126.com, chemist@126.com (S. Liu).

http://dx.doi.org/10.1016/j.carbpol.2014.07.031
0144-8617/

and alkaline peroxide mechanical pulp (APMP) (Chen et al., 2011a, 2011b; Li, Yue, & Liu, 2012; Li, Zhao, & Liu, 2013). Pulps made using these hybrid processes are known as chemical-thermomechanical pulps (CTMP). The process reportedly produces pulps with high yields and has an environmental impact approaching that of mechanical pulping. The chemical pretreatment conditions are much less vigorous (lower temperatures, shorter times, less extreme pHs) than in a chemical pulping process, because the goal is to loosen and split the fibers for easier mechanical treatment. The mechanical process leads to external fibrillation of the fibers by gradually peeling off the cell walls (P and S1 layers) and exposing the S2 layer, and also causes internal fibrillation that loosens the fiber wall. Compared with the above-mentioned cellulosic materials, CTMP seems an excellent original material for NCF production. Meanwhile, it also leads to a relatively high crystallinity (Konn, Holmbom, & Nickull, 2002; Law & Daud, 2000).

Polyvinyl alcohol (PVA) has a wide variety of applications because of its high dielectric strength, high elasticity, hydrophilic characteristics, and its ability to form good films *via* solution casting. It has a carbon chain backbone with hydroxyl groups that can act as a source of hydrogen bonding to enhance the formation of polymer complexes (Sedlarık, Saha, Kuritka, & Saha, 2006). Many researchers have dispersed cellulose fibers in the hydrophilic polymers of poly(vinyl alcohol), resulting in strong reinforcement effects (Paralikar, Simonsen, & Lombardi, 2008).

Here, using CTMP as a starting material, high intensity ultrasonication was used to prepare long, filamentous NCFs with uniform diameters. The chemical composition, morphology, crystalline structure, and thermal behavior of the NCFs and their intermediate products were characterized. The mechanical and optical properties, and the improved thermal stability in particular, of PVA composites prepared with different quantities of NCFs are also discussed in detail.

2. Experiments

2.1. Preparation of NCFs

CTMP with a brightness of 40% ISO was obtained from pine wood chips and was kindly supplied by a pulp factory in the Jilin province of China. CTMP (2 g) was mixed with an acidified $NaClO_2$ solution at 75 °C for 1 h to remove lignin content; this process was repeated five times. The resulting holocellulose fibers (Ho-CFs) were treated with 4-wt% NaOH at 90 °C for 4 h to remove hemicelluloses and residual lignin, and the residues were filtered and rinsed with distilled water until pH = 7 was obtained. The solid product was alkali-treated cellulose fibers (Al-CFs). The Al-CFs were soaked in distilled water at approximately 0.1% (w/w) solid content. An Al-CFs solution (150 mL) was placed in a 20–25-kHz ultrasonic generator (JY98-IIID, Ningbo Scientz Biotechnology Co., Ltd., Ningbo, China), equipped with a 2.5-cm-diameter cylindrical titanium alloy probe tip. The ultrasonication was conducted in an ice water bath for 30 min at an output power of 1200 W, producing a suspension of NCFs. The NCFs were separated from large bundles by centrifugation, and were freeze dried and stored at 5 °C.

2.2. Preparation of NCF-reinforced PVA films

An aqueous PVA solution (10 wt%) and an aqueous NCF water suspension (approximately 0.35 wt%) were mixed, stirred manually, and then dispersed *via* ultrasonic treatment (500 W, Tianjin Automatic Science Co., Ltd, Tianjin, China) for approximately 5 min at a power level of 85%. The mixtures were degassed in a desiccator at room temperature until films were formed; the films were then dried at 70 °C for 4 h, resulting in thicknesses of approximately 0.1 mm. Composite films with different NCF contents (0, 2, 6, 10 and 14 wt%) were prepared (denoted here as PVA, PVA/NCFs-2, PVA/NCFs-6, PVA/NCFs-10 and PVA/NCFs-14, respectively).

2.3. Chemical composition

The chemical compositions of CTMP, Ho-CFs, Al-CFs, and NCFs were determined in accordance with the standards of the Technical Association of Pulp and Paper Industry (TAPPI). The holocellulose (cellulose + hemicelluloses) content was determined as described in TAPPI T19 m-54. An acidified sodium chlorite solution method (75 °C for 1 h, 3 times) was used to obtain the holocellulose (Sun, Lawther, & Banks, 1995). The α-cellulose content of the fibers was then determined by further NaOH (17.5%, 25 ± 0.2 °C) treatment of the fibers to remove the hemicelluloses (T203os-61, α-cellulose in pulp) (Sun, Sun, Zhao, & Sun, 2004; Teixeira et al., 2010). The difference between the holocellulose and α-cellulose values yielded the hemicellulose content in the fibers. Three samples of each material were tested, and averaged values were obtained. The degree of polymerization (DP) of CTMP, Ho-CFs, and NCFs was measured using the viscosity method with an aqueous 1.0 M bis(ethylenediamine)-copper(II) hydroxide solvent, as described by Iwamoto (Iwamoto, Nakagaito, Yano, & Nogi, 2005; Iwamoto, Nakagaito, & Yano, 2007).

2.4. Characterizations

Microstructural analysis was performed using a scanning electron microscope (SEM, FEI QUANTA200 (FEI, Hillsboro, OR, USA). Prior to SEM imaging, the sample surfaces were coated with a thin layer of gold using a BAL-TEC SCD 005 sputter coater (Leica, Wetzlar, Germany) to provide electrical conductivity. Fourier transform infrared spectroscopy (FT-IR) was performed with a Magana-IR560E.S.P (Nicolet, USA) spectrometer to identify functional groups. X-ray diffraction XRD measurements were acquired on a D/max-r B X-ray diffractometer (Rigaku Corp, Tokyo, Japan) using Cu $K\alpha$ radiation. The samples were scanned over a 2θ range varying over 10−30°. The crystallinity index of cellulose materials was calculated from the height of the 2 0 0 peak (I_{200}, $2\theta = 22.6°$) and the intensity minimum between the peaks at 2 0 0 and 1 1 0 (I_{am}, $2\theta = 18°$) using the Segal method ($CI\,(\%) = (1 - I_{am}/I_{200}) \times 100$). I_{200} represents both a crystalline and an amorphous material, and I_{am} represents an amorphous material. Thermogravimetric analysis (TGA) was performed using a TGA-Q50 (TA, USA) instrument. Temperature programs for dynamic tests were run over the range 25–600 °C at a heating rate of 10 °C/min. The mechanical properties of the PVA/NCF composite films were analyzed using a RGT-20A instrument. To characterize each type of film, three samples were fabricated with lengths of 150 ± 2 mm, widths of 15 ± 0.3 mm, and thicknesses of 0.1 ± 0.05 mm. The optical transmittance was measured over 300–800 nm using a UV–vis spectrophotometer (TU-1900, Beijing Purkinje General Instrument Co., Ltd., Beijing, China).

3. Results and discussion

3.1. Chemical composition and SEM analysis

Changes in chemical composition of the fibers from different pre-treatment processes are presented in Table 1. CTMP contained a higher percentage of hemicelluloses (18.6%) and lignin (Klason lignin 21.3% and acid-insoluble lignin 2.8%), and the lowest percentage of α-cellulose (56.8%). When the fibers were subjected to $NaClO_2$ treatment, the lignin content of the Ho-CFs decreased to 2.4%, whereas the α-cellulose and hemicellulos

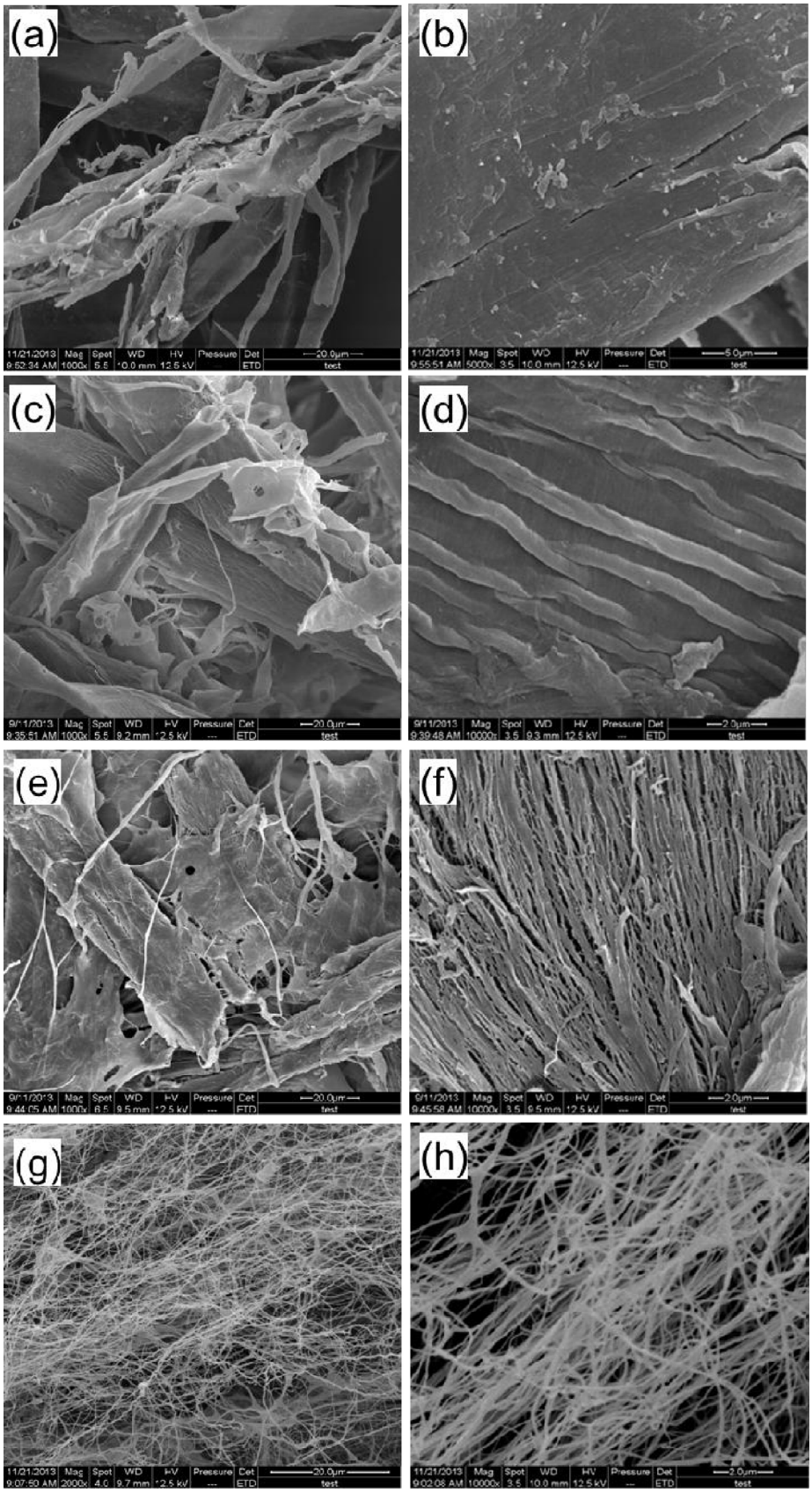

Fig. 1. SEM images of (a and b) raw CTMP; (c and d) fibers after acidified sodium chlorite treatment (Ho-CFs); (e and f) fibers after alkali-treated (Al-CFs); and (g and h) NCFs.

Table 1
Chemical compositions and DP of CTMP, Ho-CFs, Al-CFs and NCFs.

Material	α-Cellulose (%)	Hemicelluloses (%)	Klason lignin (%)	Acid-insoluble lignin (%)	DP
CTMP	56.8 ± 1.4	18.6 ± 0.8	21.3 ± 1.5	2.8 ± 0.2	1535 ± 14
Ho-CFs	69.4 ± 1.7	25.4 ± 1.3	2.4 ± 0.1	–	1210 ± 12
Al-CFs	84.3 ± 2.5	13.2 ± 0.5	–	–	1016 ± 10
NCFs	86.5 ± 2.2	11.6 ± 0.3	–	–	865 ± 8

content increased to 69.4 and 25.4%, respectively. After NaOH treatment, the α-cellulose content of the Al-CFs increased to 84.3%, resulting in highly purified cellulose fibers. The cellulose fiber structure changed as a function of the removal of the primary components (Fig. 1). The unique chemical-mechanical effects of CTMP on raw cellulose fibers were because of a special pulping process in which caustics were used to soften wood chips before mechanical treatment. After mechanical treatment, the cohesive forces of the fiber decreased and the fibers become looser and softer. The S1-layer was peeled off into flakes (Fig. 1a) to enhance the swelling and the absorption capability, making it more easily permeable to $NaClO_2$ and NaOH solutions. This also decreases the treatment time and the amounts of chemical reagents. However, there are no detailed changes of the CTMP surface that can be observed in Fig. 1b; it exhibited some wrinkling, while other local areas exhibited relative smoothness (Fig. 1c and d). The fiber structure was also maintained after $NaClO_2$ treatment removed most of the lignin. After NaOH treatment was performed to remove most hemicelluloses and residual lignin, fibrillation on the cellulose surface can be clearly observed (Fig. 2e and f). These changes were favorable to the subsequent high intensity ultrasonic treatment that can concentrate ultrasonic stress for efficient defibrillation.

Long filamentous NCFs are shown in Fig. 1g and h. It is interesting to note that they formed a network structure. When the dispersing aqueous medium was removed by freeze-drying, the NCFs were left interlaced to each other. About 80% had diameters ranging from 50 to 120 nm (Fig. 3e). Moreover, as listed in Table 1, the DP of the NCFs was 865, a decrease of 43.6% relative to that of CTMP. This revealed that more long-chain polysaccharides of cellulose were maintained compared with traditional acid hydrolysis methods during chemical and ultrasonic processing (Bondeson, Mathew, & Oksman, 2006). The scission of cellulose polymers results from solvodynamic shear created by ultrasonic cavitation. A liquid jet propagates toward the cellulose surface at a velocity of several hundred meters per second, and makes violent contact, resulting

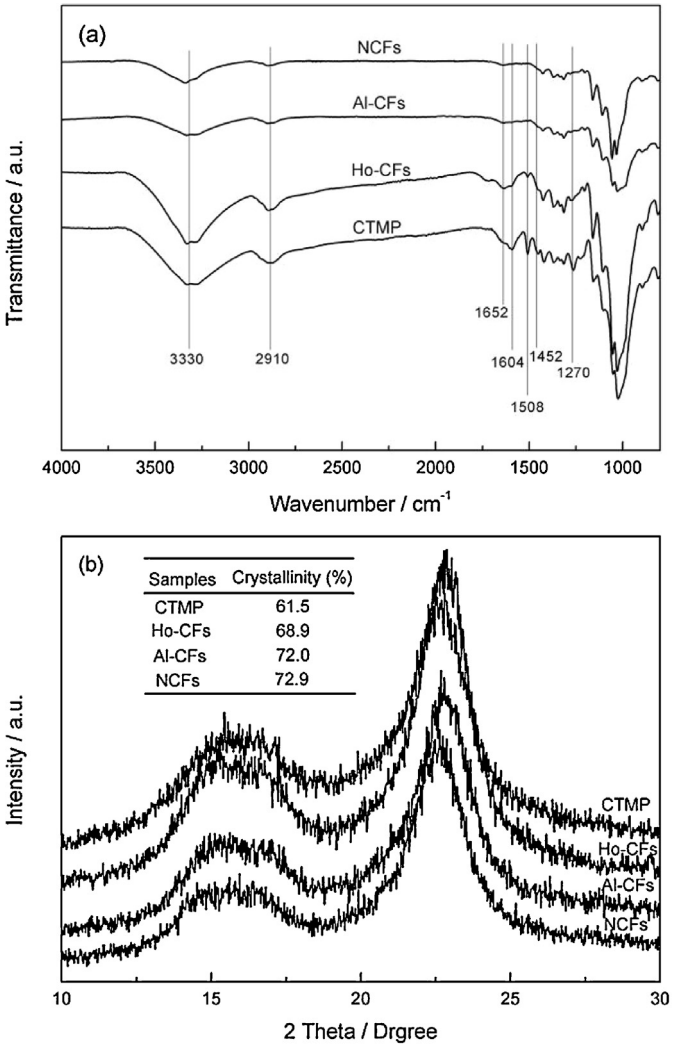

Fig. 2. (a) FT-IR spectra of CTMP, Ho-CFs, Al-CFs, and NCFs. (b) X-ray diffraction patterns of the same.

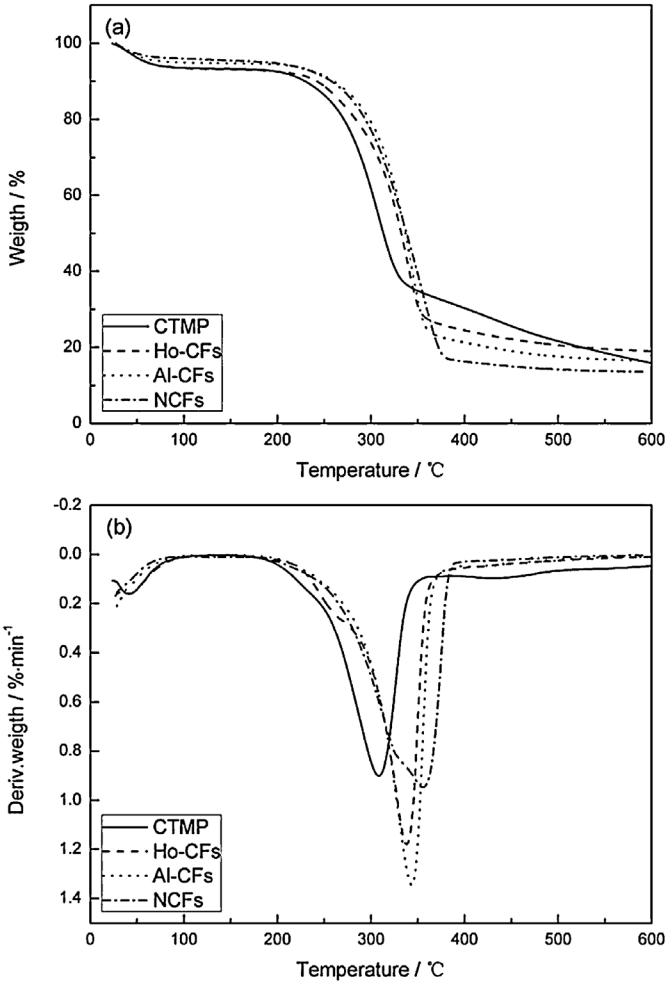

Fig. 3. TGA (a) and DTG (b) curves for CTMP, Ho-CFs, Al-CFs and NCFs.

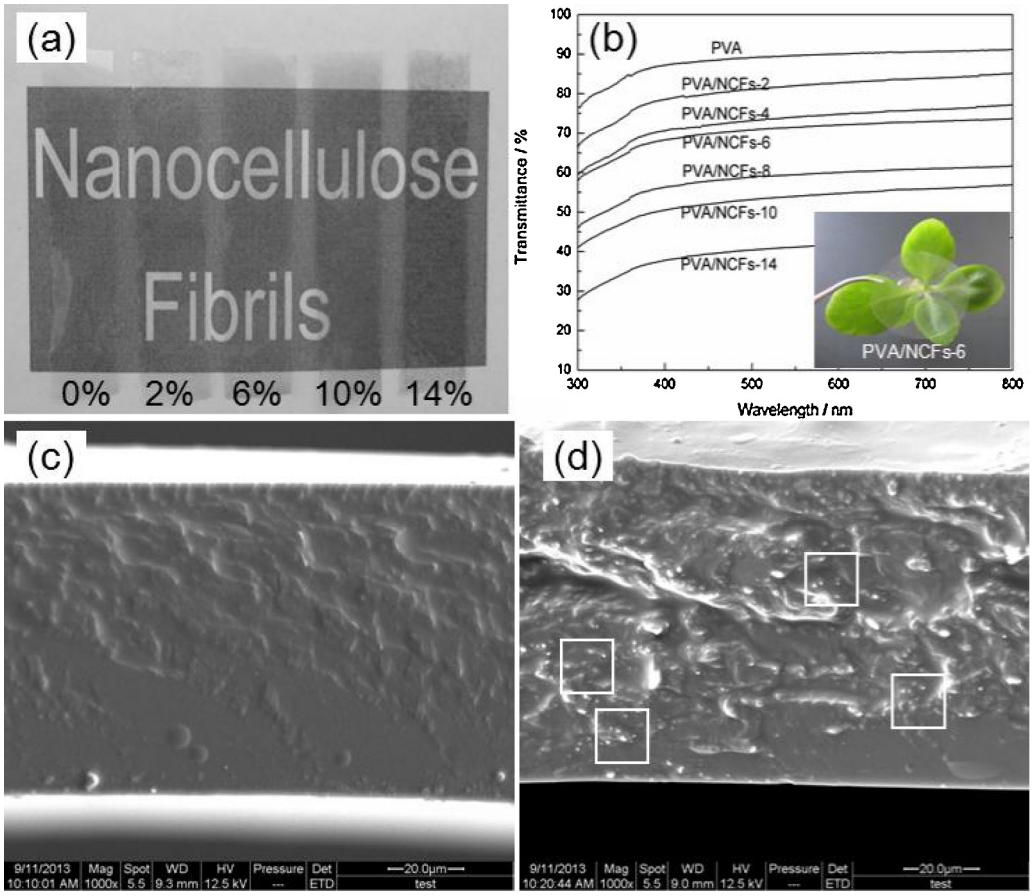

Fig. 4. (a) optical photo, (b) transmittance property curves for PVA/NCF composites, (c) SEM image of PVA, and (d) SEM image of PVA/NCFs-6 composites.

in significant morphology changes (Caruso et al., 2009). The long web-like and filamentous NCFs could be used in a variety of applications, such as reinforced nanocomposites, advanced functional materials, and membrane filters.

3.2. FT-IR and XRD analysis of CTMP, Ho-CFs, Al-CFs and NCFs

FT-IR spectra of CTMP, Ho-CFs, Al-CFs and NCFs are plotted in Fig. 2a. The 1508 and 1452 cm^{-1} peaks of CTMP are attributed to the aromatic ring C=C stretching vibrations and the C—H deformation vibrations of lignin, respectively (Sain & Panthapulakkal, 2006; Sun, Tomkinson, Wang, & Xiao, 2000). The intensity of these peaks almost disappeared for Ho-CFs, because of lignin removal. The peaks at 1270 cm^{-1} for CTMP and Ho-CFs are attributed to the C—O of guaiacyl, while the peaks at 1604 cm^{-1} for CTMP and Ho-CF are from the aromatic rings of lignin (Lebo & Lonsky, 1990; Imsgard, Falkehag, & Kringstad, 1971). The two peaks disappeared for Al-CFs and NCFs, which is attributed to the removal lignin. These results confirmed the data summarized in Table 1. After ultrasonic treatment, the spectrum of the NCFs was almost the same as that of the Al-CFs. This fact indicated that more hemicelluloses and lignin were removed during the treatment with $NaClO_2$ and NaOH, and that the original molecular structure of cellulose was maintained even after these components were removed and after the ultrasonic treatments.

Fig. 2b plots X-ray diffraction profiles and lists the crystallinity of the CTMP, Ho-CFs, Al-CFs, and NCFs. All samples had diffraction peaks at $2\theta = 16.5^\circ$ and 22.5°, and had the typical cellulose I pattern (Nishiyama, Sugiyama, Chanzy, & Langan, 2003). The crystallinity of CTMP was 61.5%. After $NaClO_2$ treatment, the crystallinity of Ho-CFs increased to 68.9% because of lignin removal. The crystallinity of Al-CFs increased to 72.0% because of hemicellulose removal from amorphous regions. After ultrasonication, the crystallinity of NCFs increased to 72.9%; and from the NCF XRD profiles, it can be observed that the intensities of the amorphous and crystalline areas all decreased. Therefore, both amorphous and crystalline cellulose were removed. The increased crystallinity may owed to a slower decline in the proportion of crystalline areas (Li et al., 2012, 2013). The effect of ultrasonication in heterogeneous systems is primarily the consequence of cavitation. In the CF-water system, both the crystalline and amorphous regions were subjected to intense collisions (Cintas & Luche, 1999). It can be concluded that on the CF surface, the intense physical stresses cause hydrogen bond breakage between the CF microfibers that are then defibrillated to NCFs. The high crystallinity of NCFs could provide better strength in composite materials (Sakurada, Nukushina, & Ito, 1962).

3.3. TG and DTG analysis

Thermogravimetric (TG) and derivative TG (DTG) curves for CTMP, Ho-CFs, Al-CFs, and NCFs (Fig. 3) showed that, for all samples, a small weight loss corresponding to the evaporation of absorbed water was observed at low temperatures (<110 °C). The primary degradation of CTMP occurred at 201.1 °C, and the maximum degradation was observed at 308.2 °C because of cellulose pyrolysis. Owing to the removal of lignin, the initial degradation and the main degradation peak of Ho-CFs increased to 208.4 °C and 338.1 °C, respectively. After most of the hemicelluloses were removed in the NaOH treatment, the maximum degradation temperature for the Al-CFs was shifted to a higher temperature (342.9 °C). These results show that removal of hemicelluloses could improve the thermal stability of cellulose fibers. For NCFs, the maximum degradation

Table 2
Onset temperature and T_{max} (degradation temperature) of pure PVA and PVA/NCF composites with NCF weight contents of 2, 6, 10, and 14%.

Sample	First process	Second process		Third process	
	T_{max} (°C)	Onset temperature (°C)	T_{max} (°C)	Onset temperature (°C)	T_{max} (°C)
PVA	93.4	181.7	248.7	342.7	432.7
PVA/NCFs-2	93.8	182.2	253.6	343.9	431.7
PVA/NCFs-6	102.5	184.6	262.5	346.2	430.6
PVA/NCFs-10	98.3	189.9	265.6	346.7	428.1
PVA/NCFs-14	98.6	184.7	253.9	339.5	430.6

was observed at 355.4 °C. The starting and maximum degradation temperatures for NCFs were all significantly higher than those of CTMP, which indicated that the thermal stability of the NCFs increased. The excellent thermal properties are suitable for thermoplastics, for which high processing temperatures are generally needed (Glasser, Taib, Jain, & Kander, 1999).

3.4. Optical properties and SEM analysis of PVA/NCF composites

Fig. 4a shows a photograph of PVA/NCF composite films with 0, 2, 6, 10, and 14 wt% NCFs. The optical transmittances of the composites were largely dependent on the dispersion of the NCFs in the PVA matrix. The letters in the background could be clearly seen through the films, which indicated transparency. However, the films became increasingly opaque with increasing NCF contents. When the transmittances of pure PVA and the PVA/NCF composites are plotted as shown in Fig. 4b, the transmittance decreased with increasing NCF content. When the NCF content was 2, 4 and 6 wt%, the films show transparent, and the transmittance was 85%, 77% and 73%, respectively. When the NCFs content was increased to 8 wt%, the transmittance decreased from 91 to 61%. Along with the increasing of NCF content was 10%, the transmittance decreased significantly to 56%, owing to the poor dispersion of the NCFs. As shown in Fig. 4c, the surface of the PVA/NCFs-6 composites was smooth. A SEM cross-sectional image of the fracture surface of a PVA/NCF-6 composite (Fig. 4d) shows that the dispersion of the NCFs in the PVA was uniform.

3.5. Thermal properties of the PVA/NCF composites

Fig. 5 shows TGA and DTG curves for pure PVA and for PVA/NCF composites. According to the DTG curves, the degradation of pure PVA can be divided into three processes. These take place in the temperature ranges 50–181.7 °C, 181.7–342.7 °C and 342.7–500 °C. The first degradation process in the PVA/NCF composite began at a slightly higher temperature than that in pure PVA. The most important result, however, was that the temperature of the second degradation process in PVA/NCF was higher than that of pure PVA, which indicates an increased PVA/NCF thermal stability. Combined with results in Table 2, it can be seen that with the introduction of NCFs in PVA, there are higher maximum decomposition temperatures in the first process 0.4–9.1 °C, and the maximum decomposition temperatures of second process increased 4.9–16.9 °C. The latter indicated that adding a small portion of NCF dramatically improved the thermal stability of PVA/NCF.

3.6. Mechanical properties of PVA/NCF composites

Fig. 6 shows the results of tensile strength and Young's modulus tests on neat PVA and PVA/NCF composites with 2, 4, 6, 8,

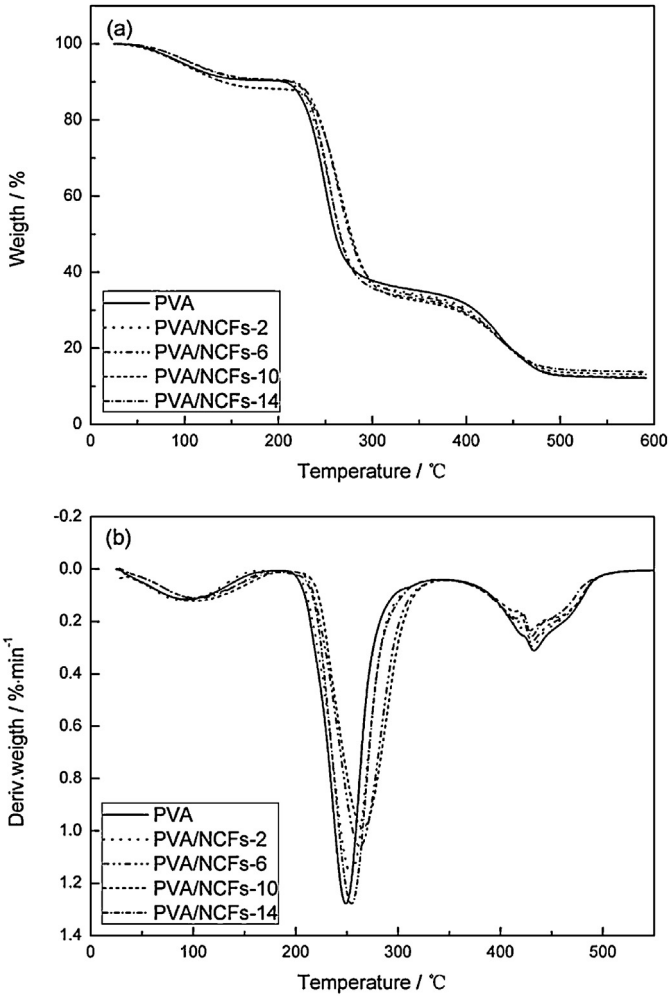

Fig. 5. TGA (a) and DTG (b) curves for the PVA and PVA/NCF composite.

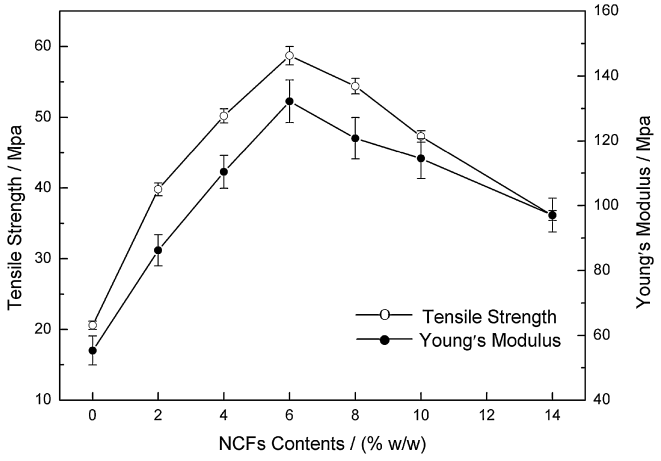

Fig. 6. Mechanical property curves for PVA/NCF composites.

10, and 14 wt% NCF. The mechanical properties increased with the increasing of NCF content from 2 to 6 wt%. When the NCF content was 6%, the tensile strength and Young's modulus of the PVA composites reached maximum values, which were 2.8 and 2.4 times larger than that of neat PVA, respectively. This indicated a strong reinforcement of the PVA matrix with addition of the NCFs. For NCF content greater than 6 wt%, the tensile strength and Young's modulus exhibited a declining trend; this may be because of decreased NCF dispersion, making the PVA composites more fragile. Thus, the aggregation of NCFs in PVA caused local concentrations of stress, and tensile failure occurred more readily. Combined with the thermal and transmittance results, these mechanical results lead to the conclusion that a NCF content of 6 wt% is optimal for PVA composites.

4. Conclusions

We have demonstrated a facile preparation of long, filamentous NCFs with 50–120-nm diameters from CTMP by using high intensity ultrasonication. The NCFs were mainly cellulose because the cellulose I crystal structure remained following the removal of lignin and parts of the hemicelluloses during the chemical process. The resulting NCFs exhibited higher crystallinity (72.9%) compared with that of CTMP (61.5%). The main thermal degradation temperature of the NCFs (355.4 °C) was higher than that of CTMP (308.2 °C) owing to removal of the lignin and parts of the hemicelluloses. Because of the excellent thermal stability of the NCFs, the maximum temperature of the second degradation process for PVA/NCF was increased by 13.8 °C for a NCF content of 6 wt%. Thus, the thermal stability of PVA/NCF increased significantly. The tensile strength and Young's modulus of the PVA/NCF composites were also significantly improved, with values 2.8 and 2.4 times larger than that of neat PVA, respectively. Finally, the composites also retained excellent transparency.

Acknowledgments

This project was supported financially by the Research Fund for the Fundamental Research Funds for the Central Universities (DL13BBX14, 2572014EB01), the National Natural Science Foundation of China (No. 31170545) and National Key Technology R&D Program (2012BAD32B04).

References

Abdul Khalil, H. P. S., Bhat, A. H., & Ireana Yusra, A. F. (2012). Green composites from sustainable cellulose nanofibrils: A review. *Carbohydrate Polymers*, *87*, 963–979.
Alemdar, A., & Sain, M. (2008). Isolation and characterization of nanofibers from agricultural residues-wheat straw and soy hulls. *Bioresource Technology*, *99*, 1664–1671.
Aliyu, M., & Hepher, M. J. (2000). Effects of ultrasound energy on degradation of cellulose material. *Ultrasonics Sonochemistry*, *7*, 265–268.
Bhatnagar, A., & Sain, M. J. (2005). Processing of cellulose nanofiber-reinforced composites. *Reinforced Plastics Composites*, *24*(12), 1259–1268.
Bondeson, D., Mathew, A., & Oksman, K. (2006). Optimization of the isolation of nanocrystals from microcrystalline cellulose by acid hydrolysis. *Cellulose*, *13*, 171–180.
Bruce, D. M., Hobson, R. N., Farrent, J. W., & Hepworth, D. G. (2005). High performance composites from low-cost plant primary cell walls. *Composites A: Applied Science and Manufacturing*, *36*, 1486–1493.
Caruso, M. M., Davis, D. A., Shen, Q. L., Odom, S. A., Sottos, N. R., White, S. R., & Moore, J. S. (2009). Mechanically-induced chemical changes in polymeric materials. *Chemical Reviews*, *109*(11), 5755–5798.
Chakraborty, A., Sain, M., & Kortschot, M. (2005). Cellulose microfibrils: A novel method of preparation using high shear refining and cryocrushing. *Holzforschung*, *59*, 02–107.
Cheng, Q. Z., Wang, S. Q., & Han, Q. Y. (2010). Novel process for isolating fibrils from cellulose fibers by high-intensity ultrasonication. II. Fibril characterization. *Journal of Applied Polymer Science*, *115*, 2756–2762.
Cheng, Q. Z., Wang, S. Q., & Rials, T. G. (2009). Poly(vinyl alcohol) nanocomposites reinforced with cellulose fibrils isolated by high intensity ultrasonication. *Composites A: Applied Science and Manufacturing*, *40*(2), 218–224.
Chen, W. S., Yu, H. P., & Liu, Y. X. (2011). Preparation of millimeter-long cellulose I nanofibers with diameters of 30–80 nm from bamboo fibers. *Carbohydrate Polymers*, *86*, 453–461.
Chen, W. S., Yu, H. P., Liu, Y. X., Chen, P., Zhang, M. X., & Hai, Y. F. (2011). Individualization of cellulose nanofibers from wood using high-intensity ultrasonication combined with chemical pretreatments. *Carbohydrate Polymers*, *83*, 1804–1811.
Cintas, P., & Luche, J. L. (1999). Green chemistry: The sonochemical approach. *Green Chemistry*, *1*, 115–125.
Cote, G. L., & Willet, J. L. (1999). Thermomechanical depolymerization of dextran. *Carbohydrate Polymers*, *39*, 119–126.
Filson, P. B., & Dawson-Andoh, B. E. (2009). Sono-chemical preparation of cellulose nanocrystals from lignocellulose derived materials. *Bioresource Technology*, *100*, 2259–2264.
Glasser, W. G., Taib, R., Jain, R. K., & Kander, R. (1999). Fiber-reinforced cellulosic thermoplastic composites. *Journal of Applied Polymer Science*, *73*, 1329–1340.
Gronroos, A., Pirkonen, P., & Ruppert, O. (2004). Ultrasonic depolymerization of aqueous carboxymethylcellulose. *Ultrasonics Sonochemistry*, *11*, 9–12.
Habibi, Y., Lucia, L. A., & Rojas, O. J. (2010). Cellulose nanocrystals: Chemistry, self-assembly, and applications. *Chemical Reviews*, *110*, 3479–3500.
Imsgard, F., Falkehag, I., & Kringstad, K. P. (1971). On possible chromophoric structures in spruce wood. *Tappi*, *54*(10), 1680–1684.
Iwamoto, S., Nakagaito, A. N., Yano, H., & Nogi, M. (2005). Optically transparent composites reinforced with plant fiber-based nanofibers. *Applied Physics A: Materials Science and Processing*, *81*, 1109–1112.
Iwamoto, S., Nakagaito, A. N., & Yano, H. (2007). Nano-fibrillation of pulp fibers for the processing of transparent nanocomposites. *Applied Physics A: Materials Science and Processing*, *89*(2), 461–466.
Kasaai, M. R., Arul, J., & Charlet, G. (2008). Fragmentation of chitosan by ultrasonic irradiation. *Ultrasonics Sonochemistry*, *15*, 1001–1008.
Konn, J., Holmbom, B., & Nickull, O. (2002). Chemical reactions in chemimechanical pulping: Material balances of wood components in a CTMP process. *Journal of Pulp and Paper Science*, *28*, 395–399.
Law, K. N., & Daud, W. R. W. (2000). CMP and CTMP of a fast-growing tropical wood: *Acacia mangium*. *Tappi Journal*, *83*, 1–7.
Lebo, S. E., & Lonsky, W. F. W. (1990). The occurrence and light-induced formation of ortho-quinonoid lignin structures in white spruce refiner pulp. *Journal of Pulp and Paper Science*, *16*(5), J139–J143.
Leitner, J., Hinterstoisser, B., Wastyn, M., Keches, J., & Gindl, W. (2007). Sugar beet cellulose nanofibril-reinforced composites. *Cellulose*, *14*, 419–425.
Liu, H., Du, Y. M., & Kennedy, J. F. (2007). Hydration energy of the 1, 4-bonds of chitosan and their breakdown by ultrasonic treatment. *Carbohydrate Polymers*, *68*, 598–600.
Li, W., Yue, J. Q., & Liu, S. X. (2012). Preparation of nanocrystalline cellulose via ultrasound and its reinforcement capability for poly(vinyl alcohol) composites. *Ultrasonics Sonochemistry*, *19*, 479–485.
Li, W., Zhao, X., & Liu, S. X. (2013). Preparation of entangled nanocellulose fibers from APMP and its magnetic functional property as matrix. *Carbohydrate Polymers*, *94*, 278–285.
Nakagaito, A. N., & Yano, H. (2004). The effect of morphological changes from pulp fiber towards nano-scale fibrillated cellulose on the mechanical properties of high strength plant fiber based composites. *Applied Physics A: Materials Science & Processing*, *78*, 547–552.
Nishiyama, Y., Sugiyama, J., Chanzy, H., & Langan, P. (2003). Crystal structure and hydrogen bonding system in cellulose Iα from synchrotron X-ray and neutron fiber diffraction. *Journal of the American Chemical Society*, *125*(47), 14300–14306.
Pandey, J. K., Misra, M., Mohanty, A. K., Drzal, L. T., & Singh, R. P. (2005). Recent advances in biodegradable nanocomposites. *Journal of Nanoscience and Nanotechnology*, *5*(4), 497–526.
Paralikar, S. A., Simonsen, J., & Lombardi, J. (2008). Poly(vinyl alcohol)/cellulose nanocrystal barrier membranes. *Journal of Membrane Science*, *320*, 248–258.
Phong, N. T., Gabr, M. H., Okubo, K., Chuong, B., & Fujii, T. (2013). Enhancement of mechanical properties of carbon fabric/epoxy composites using micro/nano-sized bamboo fibrils. *Materials and Design*, *47*, 624–632.
Portenlanger, G., & Heusinger, H. (1997). The influence of frequency on the mechanical and radical effects for the ultrasonic degradation of dextranes. *Ultrasonics Sonochemistry*, *4*, 127–130.
Sain, M., & Panthapulakkal, S. (2006). Bioprocess preparation of wheat straw fibers and their characterization. *Industrial Crops and Products*, *23*(1), 1–8.
Sakurada, I., Nukushina, Y., & Ito, T. (1962). Experimental determination of the elastic modulus of crystalline regions in oriented polymers. *Journal of Polymer Science*, *57*(165), 651–660.
Sedlarık, V., Saha, N., Kuritka, I., & Saha, P. (2006). Characterization of polymeric biocomposite based on poly(vinyl alcohol) and poly(vinyl pyrrolidone). *Polymer Composites*, *27*, 147–152.
Shih, Y. F., & Huang, C. C. (2011). Polylactic acid (PLA)/banana fiber (BF) biodegradable green biocomposites. *Journal of Polymer Research*, *18*, 2335–2340.
Stenstad, P., Andresen, M., Tanem, B. S., & Stenius, P. (2008). Chemical surface modification of microfibrillated cellulose. *Cellulose*, *15*, 35–45.
Sun, J. X., Sun, X. F., Zhao, H., & Sun, R. C. (2004). Isolation and characterization of cellulose from sugarcane bagasse. *Polymer Degradation and Stability*, *84*, 331–339.
Sun, R. C., Lawther, J. M., & Banks, W. B. (1995). Influence of alkaline pre-treatments on the cell wall components of wheat straw. *Industrial Crops and Products*, *4*, 127–145.
Sun, R. C., Tomkinson, J., Wang, Y. X., & Xiao, B. (2000). Physico-chemical and structural characterization of hemicelluloses from wheat straw by alkaline peroxide extraction. *Polymer*, *41*(7), 2647–2656.

Suslick, K. S., Choe, S. B., Cichowlas, A. A., & Grinstaff, M. W. (1991). Sonochemical synthesis of amorphous iron. *Nature*, *353*, 414–416.

Svagan, A. J., Samir, M. A. S. A., & Berglund, L. A. (2008). Biomimetic foams of high mechanical performance based on nanostructured cell walls reinforced by native cellulose nanofibrils. *Advanced Materials*, *20*, 1263–1269.

Teixeira, E. M., Corrêa, A. C., Manzoli, A., Leite, F. L., Oliveira, C. R., & Mattoso, L. H. C. (2010). Cellulose nanofibers from white and naturally colored cotton fibers. *Cellulose*, *17*, 595–606.

Tischer, P. C. S. F., Sierakowski, M. R., Westfahl, H., & Tischer, C. A. (2010). Nanostructural reorganization of bacterial cellulose by ultrasonic treatment. *Biomacromolecules*, *11*(5), 1217–1224.

Vodeniãarová, M., Drímaloví, G., Hromádková, Z., Malovíková, A., & Ebringerová, A. (2006). Xyloglucan degradation using different radiation sources: A comparative study. *Ultrasonics Sonochemistry*, *13*, 157–164.

Wang, B., & Sain, M. (2007). Dispersion of soybean stock-based nanofiber in a plastic matrix. *Polymer International*, *56*, 538–546.

Wang, S. Q., & Cheng, Q. Z. (2009). A novel process to isolate fibrils from cellulose fibers by high-intensity ultrasonication, Part 1: Process optimization. *Journal of Applied Polymer Science*, *113*, 1270–1275.

Wegner, T. H., & Jones, P. E. (2006). Advancing cellulose-based nanotechnology. *Cellulose*, *13*, 115–118.

Zhang, W., Zhang, Y. A., Lu, C. H., & Deng, Y. L. (2012). Aerogels from crosslinked cellulose nano/micro-fibrils and their fast shape recovery property in water. *Journal of Materials Chemistry*, *22*, 11642–11650.

Zhao, H., Feng, X., & Gao, H. (2007). Ultrasonic technique for extracting nanofibers from nature materials. *Applied Physics Letters*, *90*, 073112.